Physical Science International Journal
5(4): 230-240, 2015, Article no.PSIJ.2015.024
ISSN: 2348-0130

SCIENCEDOMAIN *international*
www.sciencedomain.org

New Metrology Approach for Single Molecular Device: Probing of Molecular Energy Gap by Electrical and Optical Measurements

V. Andrei Pakoulev[1], Tatjana N. Kopylova[2], Yu. Sergey Nikonov[2], N. Evgeny Telminov[2] and Vladimir Burtman[3*]

[1]Department of Chemistry, University of Wisconsin, 1101 University Ave, Madison, WI 53706-1322, USA.
[2]Siberian Physics and Technical Institute Tomsk State University, Tomsk, Novosobornaya-1, Russia, 634050.
[3]Department of Geology and Geophysics, University of Utah, 135 S. 1460 E, Salt Lake City, UT 84112-0111, USA.

Authors' contributions

This work was carried out in collaboration between all authors. All authors made an equal contribution into this study. All authors read and approved the final manuscript.

Article Information

DOI: 10.9734/PSIJ/2015/14438
Editor(s):
(1) Alexander A. Kaminskii, Shubnikov Institute of Crystallography, Russian Academy of Sciences, Russia.
(2) Stefano Moretti, School of Physics & Astronomy, University of Southampton, UK.
Reviewers:
(1) Kasem K. Kasem, School of Sciences, Indiana University Kokomo, USA.
(2) Anonymous, India.
(3) Jiao Chen, Chemistry Department, New Mexico Highlands University, USA.
(4) Anonymous, Brazil.
Complete Peer review History: http://www.sciencedomain.org/review-history.php?iid=835&id=33&aid=7592

Original Research Article

Received 30th September 2014
Accepted 6th December 2014
Published 1st January 2015

ABSTRACT

We report on electrical and optical measurements to probe the energy gap in single molecular devices. The closeness of energy of the high occupied molecular orbital - low unoccupied molecular orbital (HOMO-LUMO) energy gap was detected by electric (Φ_B^{Σ}) and optic measurements (Δ_o), $\Phi_B^{\Sigma} \approx \Delta_o$. The 'electrical gap', Φ_B^{Σ}, consists of sum of two barriers, Φ_B^{LUMO} and Φ_B^{HOMO}, for tunneling of electrons and holes through molecular barrier correspondingly, in devices with a different pair of electrodes at low biases and difference in work function, Δ_{WF}, between these metal electrodes: $\Phi_B^{\Sigma} = \Phi_B^{LUMO} + \Phi_B^{HOMO} + \Delta_{WF}$. We fabricated and tested two devices with a pair of gold (Au) and aluminum (Al) electrodes to find Φ_B^{HOMO} (Φ_B^{Au}) and Φ_B^{LUMO} (Φ_B^{Al}) using Simmons

**Corresponding author: Email: vlad.burtman@utah.edu, vlad.burtman@gmail.com;*

tunneling model. The symbols Φ_B^{LUMO} and Φ_B^{HOMO} signify energy difference between HOMO and LUMO levels in a molecular system with respect to the Au and Al electrode's Fermi level. Comparison of Φ_B^{Σ} and Δ_o can identify presence of electrically active molecules between electrodes in nanoscale devices.

Keywords: Molecular nanoelectronics; nanowires; energy gap; tunneling models; molecular junctions; self-assembled-monolayer.

1. INTRODUCTION

Measurements of electronic properties of nanoscale and molecular junctions do not provide direct structural information about molecular junction [1]. Indeed, direct experimental correlation between structure and electronic properties, observed in monoatomic Au wires [2], is not feasible for metal-molecule-metal junctions, at least for carbon-based organic molecules [1]. Therefore, experimental studies of molecular junctions require additional structure-oriented experiments, such as combined transport studies under stimuli of mechanical force, optical illumination, and thermal gradients [1]. These techniques that can provide some information about structure of molecular junction are barely accessible for many experimental groups. The present work proposes asimpler technique for characterization of molecular junctions based on evaluation of molecular energy gaps.

Currently, the most accessible approaches to analysis of a single molecular transport are the phenomenological WKB-derived direct tunneling model at low bias and field emission tunneling at higher biases traditionally referred as Simmons model [3-6] and Flower-Nordhaim (FN) tunneling. These approximate, phenomenological models present a necessary step for quantifying the increasing amount of molecular transport data [1]. Crossover between trapezoidal barriers regime and triangular barrier regime in the Simmons model has been studied in the case of molecular junctions [7-11]. This crossover methodology has potential to become a metrology tool for analysis of molecular nanojunctions due to the correlation between energy scale of transition point (V_{trans}) and optical offset between Fermi Energy Level (E_F) and nearest molecular orbital (MO).

The optical offset can be detected independently from ultraviolet photoelectron spectroscopy (UPS) spectra. This combination of electrical and an optical measurements over a wide range of molecular devices provides the necessary evidence of reliability of this "crossover" technique. The simultaneous analysis of electrical and optical properties is a useful approach to study transportin molecular nanosystems [12].

In this communication we study optical and electrical probing of molecular gap. This approach assumes that Simmons-type tunneling is the main transport mechanism in molecular diodes at low biases, when applied bias, V, is less than value of Simmons barrier, Φ_B, i.e.: $V < \Phi_B$ [3,13]. We also assume that device with Au electrodes has a hole conductivity (since E_F^{Au} is in the HOMO proximity) and device with Al electrodes has an electron conductivity (since E_F^{Al} is in the LUMO proximity). Tunneling through HOMO and LUMO molecular orbitals is determined by values of Φ_B^{LUMO} and Φ_B^{HOMO} barriers between these molecular orbitals and E_F of electrodes. For device with Au and Al electrodes those barriers are designated as Φ_B^{Au} and Φ_B^{Al} correspondingly. Φ_B^{Au} and Φ_B^{Al} barriers can be derived from conductivity measurements by using Simmons model at low biases. Knowledge of Φ_B^{Au} and Φ_B^{Al} values and difference in work function, Δ_{WF}, between Au and Al metal electrodes allows us to evaluate gap between HOMO and LUMO for single molecular junction by summation of Φ_B^{Au} and Φ_B^{Al} and Δ_{WF} values. We designate the HOMO-LUMO gap that can be derived from electrical measurement as Φ_B^{Σ}. The same gap can be found by optical measurements. The goal of this paper is to compare the Φ_B^{Σ} to the optical gap Δ_o [14].

There is 1 eV difference in work function, Δ_{WF}, between Au and Al [15]. Therefore, E_F of Al (~ 4.1 eV) should be closer to LUMO than E_F of Au (~ 5.2 eV), which should result in electron transport through E_F-LUMO barrier for Al electrodes, and holes transport through HOMO-E_F barrier in case of Au electrodes [16]. Note that the tunneling model is developed for HOMO-mediated tunneling for holes and LUMO mediated tunneling for electrons, but suggested 'gap' model also applies to LUMO-mediated hole

tunneling and HOMO-mediated electron tunneling. What is important in this experiment is that Φ_B^{Au} and Φ_B^{Al} should correspond to tunneling of charge carriers with opposite charge. Φ_B^{Au} and Φ_B^{Al} can be obtained from the electrical measurements using Simmons modeling of experimental data, whereas Δ_o can be defined independently from optical spectra. Δ_{WF} could be obtained from literature or while using Kelvin probe measurement [17,18].

2. ON TEMPERATURE DEPENDENCE OF TUNNELING

This study compares optical and electrical measurements of the HOMO-LUMO gap in molecular self-assembled layers. There is a well-pronounced temperature dependence of tunneling in this system, which should be clarified prior to future discussion, since analysis of tunneling parameters are critical for the main point of this paper. To justify the use of the tunneling models, three important criteria must be satisfied: (i) Exponential decay of the current with molecular length, (ii) Temperature independence, and (iii) The characteristic shape of the I-V curves. We will not report here any molecular length scale studies and assume that our results will be valid at different lengths of molecular bridge. It was indeed demonstrated that single molecular devices obey the law of the exponential current decay with increasing of molecular length [13,19].

Ideal tunneling indeed should be temperature independent and Simmons model should work only at very low temperatures. So, temperature indeed does not show up at (1) and (2) eq.'s in our manuscript. We have to note that the temperature dependent tunneling is definitely not the new phenomena. Indeed, the room temperature measurements and temperature dependent tunneling has been reported and discussed. Reed's [20,21], Allara [22] and Nowak [23] groups reported on temperature dependent transport in molecular junctions. The recent confirmation of temperature dependence of tunneling in organic devices includes Moodera's group report [24]. The nature of temperature dependence of molecular tunneling is still under discussion [25,26].

In our previous study of 2-[4-(2-mercaptoethyl)-phenyl] ethanethiol (Me-PET) as self-assembled monolayer (SAM) molecules incorporated into the matrix of molecular insulator spacers [penthane 1-thiol (PT)] at a concentration ratio of $r = 10^{-6}$ wires/spacers, [10] we found that the value of the molecular barrier, Φ_B, does not show essential temperature dependence for direct tunneling and show larger temperature dependence for the field emission tunneling (due to hopping through molecular orbital).

In that study [10] we found that the only parameter that really depends on temperature is pre-exponential G_0 factor. The number of tunneling channels increases with temperature, as reflected by change in G_0. Therefore, the current amplitude also increases, but the shape of IV remains almost the same. It is more visualized in PT samples, which do not have chemical bond with upper electrode. This phenomenon could be attributed to the well established hot-spot activation mechanism [27]. At high temperatures the number of point contacts with upper electrode increases and gives rise to the final conductivity. On the other hand, the change in G_0 due to increase of the number of conductive channels does change only the amplitude of the response, but not it's shape. This observation imposes the fact that tunneling barrier, Φ_B does not change essentially with temperature. This justifies our experimental approach even without discussion of temperature dependence of tunneling. We underline, that we do not force Φ_B temperature-independent by imposing the 'weight' of temperature dependence on alpha, or m*. The set of fitting parameter was the best one we could get from the experimental data.

We already proved [10] that the temperature dependent transport mechanisms operate in parallel to tunneling and could be separated from pure tunneling in molecular junctions. We demonstrated [10] that even if temperature activated mechanisms are in serial to molecular tunneling, it still could be separated from temperature induced phenomena. Despite the fact that tunneling should be temperature independent, the characteristics of pure molecular barriers (in devices with structures similar to those considered in our report) should be compared at high temperatures due to the fact that the injection barrier becomes transparent at higher temperature. Similar concept was used recently to compare the room temperature crossover from direct to field emission tunneling regime with optically detected barrier offset in singe molecular junctions [7-9,11].

3. MATERIALS AND METHODS

We use a nanofabrication approach, which deals with an organic monolayer with many molecules acting in parallel [28,20]. It has been demonstrated [28,29] that the organic monolayer in the nanodevice does not need to be homogeneous–it may be composed of a mixture of two different types of molecules: Conductive 'wires' and insulating 'spacers'. If electron tunneling is the main conductive mechanism, the reason for the low conductivity of 'spacers' is due to the much higher position of the energy barrier or the absence of chemical bonds with respect to electrodes. A device having properties of a single molecule device could be achieved when the fraction of molecular 'wires' is small and the device contains many independent conducting molecules acting in parallel.

This concept was used to grow the self-assembled monolayer (SAM) on metallic electrodes from a diluted mixtures of molecular wires [2-[4-(2-mercaptoethyl) phenyl] ethanethiol (Me-PET)] and molecular insulating spacers [1-pentanethiol (PT)]. Prepared precursor solutions have a concentration ratio $r = N_{Me\text{-}PET}/N_{PT}$, where $N_{Me\text{-}PET}$ and $N_{PT}$are their respective molar concentrations. The two-terminal molecular devices have been fabricated using the protocol shown schematically in Fig. 1.

In every device material of electrodes was the same. The bottom Au and Al electrodes (about 30-nm thick) was deposited on a SiO_2/Si wafer using a DVSJ/20C Denton Vacuum e-gun. The precursor mixture of Me-PET/PT was diluted with distilled toluene to a 3-mM concentration and air-free transferred into a homebuilt high-vacuum Shlenk line. The self-assembling process was continued for 12 h in an argon atmosphere at room temperature. After the SAM growth had been completed, the samples were thoroughly washed in dry toluene and annealed in vacuum for 1 h at 90ºC to remove any physisorbed precursors. The upper Au and Al electrode was then evaporated through a shadow mask in a vertical cross electrode configuration using the DV-SJ/20C e-gun at 95ºC on the sample holder. In fabricated devices the upper and bottom electrode material was the same. During the self-assembly process, we keep the ratio *r, r* = 10^{-6}. This concentration is typical for a single molecular device [29-32]. We denote this device as 'r=10^{-6} device'. In this report the conductive molecular channels are composed by Me-PET molecules. Similar studies were done using methylbenzene di-thiol (Me-BDT) molecules [29,30]. The structure of Me-PET/PT and Me-BDT/PT 'r=10^{-6} devices' are very similar. Every Si chip was constituted by three different devices, each one with an active area of about 0.5 mm^2. We have also fabricated several devices with *r* = 0 for the purpose of comparison; these devices were composed of insulated PT molecules with no molecular wires.

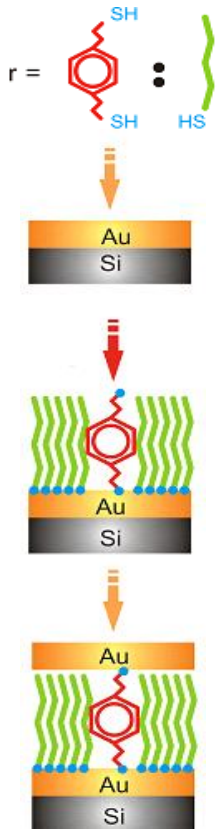

Fig. 1. SAM approach to molecular diodes. The fabrication process of SAM solid-state mixture diodes at a ratio r = 10^{-6} of molecular wires (Me-PET in red) to molecular insulators (PT in green) is shown schematically ('r = 10^{-6} device')

We have used a Keithley 236 electrometer for two terminal electrical measurements and Varian/Cary 5G spectrophotometer for recording surface reflectivity spectra. Varian/Cary 5G spectrophotometer was equipped with a custom design sample-holder for reflectivity measurement [30].

Short (~1 nm) organic molecules have substantial probability of direct tunneling due to nonzero wave function across molecular barrier.

To approximate a current-voltage response of the fabricated molecular devices, we used the Simmons model [33,34] for electron tunneling through a thin dielectric layer. This model has also been successively applied to describe an electron tunneling through a single molecule [35-37]. The model is based on the assumption that if the Fermi level of the metal electrode is closely aligned to a molecular energy level, then the effect of the other, more distant, molecular energy levels on the charge transport is negligible. Depending on position of the Fermi level, the tunneling barrier may be associated either with the highest occupied or lowest unoccupied molecular orbital (HOMO or LUMO, respectively). Simmons has derived a general expression which describes the current density versus voltage over the full range from metal-dielectric-metal to field-emission tunneling [34]. The Simmons model for organic or inorganic tunneling systems is restricted to low biases. If Φ_B^{Sim} defines the lowest Simmons barrier in the system in electron-volts and applied bias is $V < \Phi_B^{Sim}/e$ (where e is the electron charge), then the dependence of the current density J on V can be approximated as:

$$J(V) = G_0\left\{\left(\frac{2\Phi_B^{Sim}}{e} - V\right)\exp\left[-\frac{2(m_e e)^{1/2}}{h}\alpha\left(\frac{2\Phi_B^{Sim}}{e} - V\right)^{1/2} d\right]\right. \quad (1)$$
$$\left. -\left(\frac{2\Phi_B^{Sim}}{e} + V\right)\exp\left[-\frac{2(m_e e)^{1/2}}{h}\alpha\left(\frac{2\Phi_B^{Sim}}{e} + V\right)^{1/2} d\right]\right\}$$

Here, h is a Plank's constant, m_e is the electron mass, and d is the barrier width. In molecular junctions, the barrier height can be approximated by the energy offset between the electrode Fermi level and the nearest molecular orbital. For a single monolayer, barrier width d should be close to the molecular length, which has been estimated to be ~ 1 nm from the data obtained by ellipsometric measurements [31]. Parameter α provides a way to apply the model to a nonrectangular barrier and/or to account for the effective mass of the tunneling electrons. The pre-exponential factor G_0 is related to the conductivity at very low biases $V << \Phi_B/e$, when the dependence $J(V)$ becomes linear [4,38]. The G_0 is also known as an 'equilibrium conductivity' [39] and its meaning and contribution can also be extended to the field emission at high-bias range (FN mechanism) based on a different linearized presentation [7,39].

Equation (1) describes a trapezoidal barrier when the applied bias is less than the barrier height. In the zero-bias limit, the barrier is rectangular, and Eq. (1) reduces to

$$J(V) = G_0 V \exp\left(-\frac{2d\sqrt{2m_e^*\Phi_B^{Sim}}}{h}\right) \quad (2)$$

Note that in Eq. (2) α-factor has been incorporated into the electron effective mass so that $m_e^* = \alpha^2 m_e$ [4,39]. These two presentations are equivalent because it is impossible to distinguish the contributions of α and m_e^* in Equation 1.

Table 1 summarizes tunneling parameters for 'r=0' device with Au electrodes, which is composed of PT molecules, and 'r = 10^{-6}'device, which is composed of single Me-PET molecules disperses in matrix of PT molecules.

Values of Φ_B,α and G_0 parameters are similar to the corresponding values obtained in other studies of tunneling through single molecules [3,4,13,33]. A detailed description of self-assembling approach and details of device fabrication are summarized in ref [40]. The goal was to fabricate predictable and structurally similar devices composed of solid-state mixture wires and spacer molecules with Au-Au and Al-Al electrodes in each two-terminal device. These Au and Al electrodes have essentially different work-function, which result in shift of E_F position in respect to Me-PET molecular orbitals. This might result in transport of charge carriers of opposite sign in the devices with different electrodes. This assumption enables us to test the applicability of the proposed measurement concept, $\Phi_B^{\Sigma} \approx \Delta_o$, which impose proximity of gap between molecular orbitals probed by electrical and optical measurement. Electrically probed molecular gap, Φ_B^{Σ}, is equal to sum of two barriers between Au and Al electrodes and nearest molecular orbitals, Φ_B^{Au} and Φ_B^{Al} correspondingly, and offset in work function between these metals, Δ_{WF}: $\Phi_B^{\Sigma} = \Phi_B^{Au} + \Phi_B^{Al} + \Delta_{WF}$.

The experimental response, $J(V)$, of the molecular devices with Au and Al electrodes, and the best fits with Simmons formula, Eq. (2) for low biases at different temperatures are shown in Fig. 2.

Optical spectra of the surface reflectivity of 'r = 10^{-6}'device at room temperature with a marked HOMO-LUMO optic resonance (Δ_o) are

summarized in Fig. 3. In Fig. 3 two peaks at 4.3 eV and 6.3 eV are assigned to HOMO-LUMO gap in Me-PET and PT molecules 'r = 10^{-6}'device. 4.3 eV peak is stronger and wider that 6.3 eV, presumably, due to a larger cross-section of Me-PET molecule and rotation of Me-PET molecules on substrate at room temperature [22], but both peaks are well distinguishable. Most commercial photometers are sensitive enough to record spectra of single molecules [29-31].

In Simmons range ($V << \Phi_B/e$, Eq. (1)), we use Φ_B^{Sim}, α, and G_0 as fitting parameters. The α,G_0, and Φ_B were determinate by finding the global minima of the model over the experimental data, as in ref. [36]. The temperature dependence of the fitting parameters α and G_0 are summarized in the Table 1. Parameter d was fixed at 1.0 nm, as for a Simmons fit, while for effective mass we used αvalues from Simmons fits so that $m_e^* = \alpha^2 m_e$, as has been discussed above. To develop a *two barriers approach* we focused only on the Φ_B parameter in this Letter. The decreasing of α^2 [ref.4] with a temperature was compensated by growth of G_0 factor with a temperature. Technically, this fitting approach is similar to that used previously to obtain the tunneling transport from conductivity data [23].

4. RESULTS AND DISCUSSION

A summary of the Φ_B^{Au}, Φ_B^{Al}, and Φ_B^{Σ} values resulting from the best fits for low and high biases in the temperature range 11-294 K appears in Fig. 4 [10].

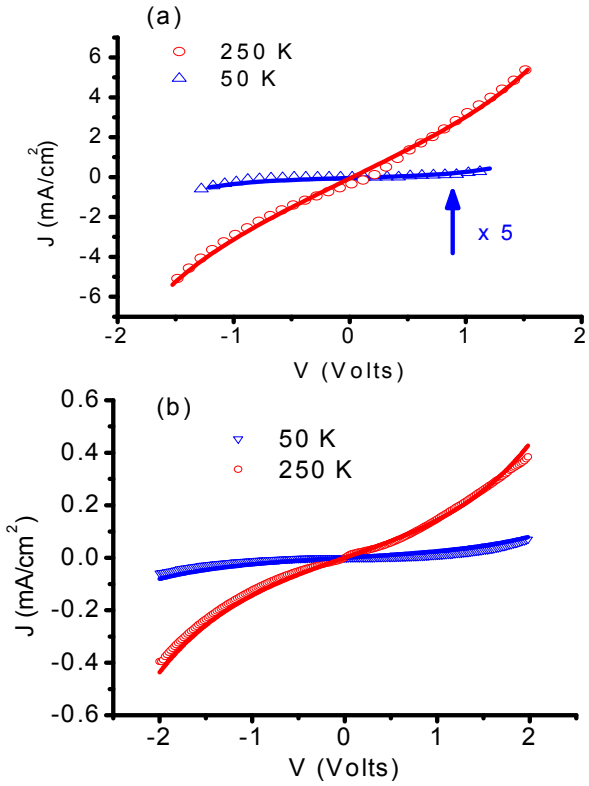

Fig. 2(a,b). Analysis of electrical transport properties in SAM diodes (Au electrodes) with r = 10^{-6} with the Simmons model fit (solid lines) over experimental data (symbols) at low temperature (50 K) and high temperature (250K) and (b) the same analysis of electrical transport properties in SAM diodes with Al electrodes at low bias [10]. Fitting results for the Simmons tunneling barrier (Φ_B) for devices with Au and Al electrodes in the temperature range 11-294 K are summarized in Fig. 4. IV's characteristics for the SAM diodes with r = 0 (only PT molecules, Au electrodes), parameters α and G_0 are summarized in Table 1

Table 1. Tunneling parameters, de-convoluted from the Simmons model at low bias

Device ID	'r=0' device			'r=10^{-6}' device		
Device structure	1-pentathiol (PT) self-assembled structure, Au electrodes			2-[4-(2-mercaptoethyl)phenyl]ethanethiol (Me-PET) self-assembled at mixing ratio r = 10^{-6} with PT molecules, Au electrodes		
T	Φ_B	α	Go	Φ_B	α	Go
K	(eV)	-	S	(eV)	-	S
15	1.600	0.970	--	1.189	0.872	--
50	1.561	0.956	5.128E-6	1.184	0.882	2.333
100	1.628	0.842	1.230E-5	1.181	0.848	2.415
150	1.492	0.779	5.523E-5	1.178	0.788	3.441
200	1.450	0.800	1.455E-4	1.195	0.734	5.132
250	1.385	0.738	0.018	1.223	0.721	11.304
294	1.345	0.669	0.057	1.261	0.723	14.347

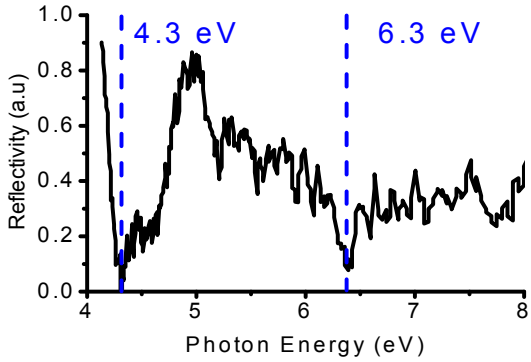

Fig. 3. Energy scale for optic measurements for 'r =10^{-6}' device shows the room temperature reflectivity optical spectra for this structure, with marked positions of HOMO-LUMO transition for the Me-PET (4.3 eV) and PT (6.3 eV) molecules

We found that the value of Φ_B has a very weak dependence on temperature, which validates this approach even at room temperatures. The best fits at low biases, averaged in all the temperature ranges, gave Φ_B^{Au} values of 1.2 ± 0.1 eV for the '$r = 10^{-6}$ device' with Au electrodes and Φ_B^{Al} values of 2.0 ± 0.1 eV for the same Me-PET with $r = 10^{-6}$, but with Al electrodes. Same analysis of the devices composed of PT molecules at only ($r = 0$) exhibit the Φ_B^{L} and α values (Table 1) are in good agreement with similar measurements by Reed et al. [41].

We fabricated '10^{-6} devices' using a to Me-PET molecules incorporated into the PT matrix with $r = 10^{-6}$. These devices have a conductivity several orders of magnitude higher than the conductivity of PT devices with $r = 0$ ('r=10^{-6}, device). The presence of both PT and Me-PET molecules in the monolayer is demonstrated by a reflectivity spectrum that has absorption bands at 6.3 and 4.3 eV. Is that possible to distinguish which molecules conduct in this heterostructure? The measurements of just the Φ_B^{Au} value (Φ_B^{Au}= 1.2 ± 0.1 eV, for Me-PET/PT device with Au electrodes) do not explain which conducting channels are responsible for conductivity this devices. On the other hand, for Me-PET/PT device with Al electrodes, we obtain Φ_B^{Al} = 2.0 ± 0.1 eV. Accounting of an offset in the work function between Au and Al electrodes, Δ_{WF}= *1 ± 0.1 eV*, yields $\Phi_B^{\Sigma}= \Phi_B^{LUMO} + \Phi_B^{HOMO}+ \Delta_{WF}$= *4.2 ± 0.3 eV.* This last value is comparable to Δ_o which is associated with the Me-PET HOMO-LUMO band gap.

We note that Φ_B^{Al} = 2.0 eV is located slightly above middle of optical gap, $\Delta_o/2$ = 2.1 eV, so the electron transport through LUMO is more favorable than hole tunneling through the HOMO. It is well-known from organic light emission diode experimental studies that both aluminum charge transfer complexes with aromatic compounds, as tris(8-quinolinolato) aluminum (Alq_3) [10], and aluminum interface with aromatic compounds facilitate an electronic transport due to low oxidation potential of these complexes. Indeed in organic devices electron conduction is preponderant for the Al (and Ca) electrodes,

while for Au (and ITO) electrodes the electron conduction is injection limited [16].

In our study, the value of Φ_B^{Σ} was very close to Δ_o. The discrepancy between these two values can be explained by accuracy of optic and electronic measurements and by the Frank-Condon principle [42], Because of momentum conservation, photon absorption is followed by an electron transition to a vibrationally excited LUMO (or HOMO) state. Electron tunneling through the molecule does not require this kind of momentum conservation. Hence, the tunneling barrier should be associated with the lowest vibronic state. The formation of mirror charge in electrode is the other possible reason of such discrepancy. The mirror charge might cause the most essential difference between Φ_B^{Σ} and Δ_o. These considerations are potential restriction for calculation of 'electrical gap' for suggested model.

This study leads to the conclusion that the electrical properties of the '$r = 10^{-6}$ device' are defined by Me-PET 'wires', whereas the contribution of the PT transport channel is negligible. The energy gap approach ($\Phi_B^{\Sigma} \approx \Delta_o$)

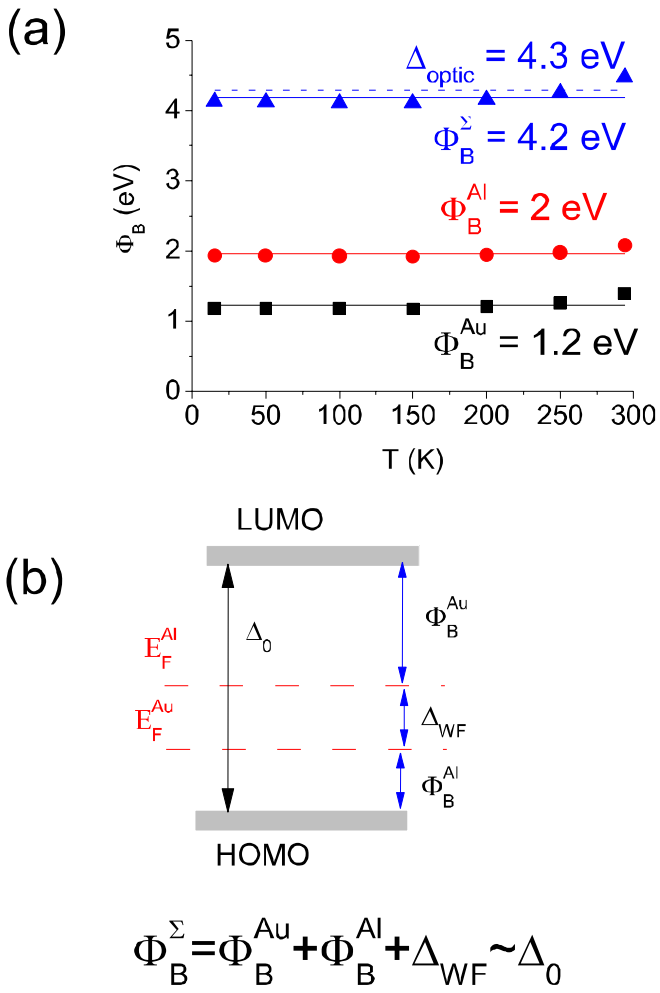

Fig. 4. (a,b) Energy scale for optic and electronic measurements for 'r =10^{-6} device'. The upper panel (a) shows the temperature dependence of low and high direct tunneling barriers, Φ_B (Φ_B^{Σ}, Φ_B^{Al} and Φ_B^{Au}). Symbols represent fitting results; solid lines represent the corresponding values averaged over the whole temperature range. The optical gap Δo obtained from the second column is plotted as a dashed blue line for comparison. The bottom panel (b) shows energy diagrams explaining the statement: ($\Phi_B^{\Sigma} \sim \Delta_0$)

remains valid for this type of heterogeneous despite differences in properties and structures of its components, as indicated in Fig. 4(b). In the '$r = 10^{-6}$ device' the lower barrier Φ_B^{HOMO} is probably associated with the distance between E_F^{Au} and the HOMO of Me-PET, whereas the higher barrier, Φ_B^{LUMO}, indicates the energy distance between E_F^{Al} and the LUMO of Me-PET. In this case, the difference between the ionization potential and Φ_B^{LUMO} (~ 2 eV) is large enough to accommodate higher LUMO states. This assumption is in agreement with other experiments for the similar samples [43] and electrodes [16].

5. CONCLUSION

We have reported on comparison of electrically and optically probed energy gap between molecular orbitals in single molecular device. The discussion is focused on determination of Simmons barriers Φ_B for the holes and electrons, Φ_B^{LUMO} and Φ_B^{HOMO}, correspondingly, in devices with same molecular structure but different electrode material. An electron or hole tunneling mechanism control transport in molecular nanodevice owing to proximity of E_F electrode to the nearest molecular orbital. This study uses Simmons modeling of experimental conductivity data to obtain the barrier for electrons and holes. Along with known difference in work function between these electrodes, Δ_{WF}, the sum of Φ_B^{LUMO} and Φ_B^{HOMO} values should be equal to electrically probed gap between molecular orbitals, Φ_B^{Σ}, $\Phi_B^{\Sigma} = \Phi_B^{LUMO} + \Phi_B^{HOMO} + \Delta_{WF}$. This value, Φ_B^{Σ}, was equal to $\Phi_B^{Al} + \Phi_B^{Au} + \Delta_{WF}$ for 'Me-PET, 10^{-6}, device, and approximately equal to value of optical gap, (Δ_o) for Me-PET molecule. Therefore, total 'electrical gap' between molecular orbitals, Φ_B^{Σ} value, could be compared with an optical HOMO-LUMO gap (Δ_o) to check there proximity, $\Phi_B^{\Sigma} \approx \Delta_o$. This estimation relies on the two barrier approximation originating from Simmons model that has been applied to devices with different work function of electrodes. The main result is the additive role of Φ_B^{LUMO}, Φ_B^{HOMO} and $\Delta_{WF,}$ which forms the 'electrically probed' molecular gap, Φ_B^{Σ}.

There has been a range of experimental and theoretical studies demonstrating that electric and optical measurements in molecular self-assembled nanostructures [1,44] can be compared in the same energy scale. Examples of these studies include inelastic spectroscopy [6], Kelvin probe measurements [17,18], optical illumination of molecular nano-structures [1] and theoretical studies of molecular energy gap [45]. Methods and approaches developed in these studies can be used to confirm presence of a specific molecule in the molecular nano-junction. Similarly to these methods, the *energy gap proximity* approach, $\Phi_B^{\Sigma} \approx \Delta_o$, described in the present article, is based on comparing optical and electrical measurements of single molecular devices in the same energy scale. Similarly to the previous studies [1,6,17,18], the *energy gap proximity* approach also provides information on the molecular structure of nanodevices. However, despite all similarities, our contribution to the research in the area of molecular nanoelectronics is in the fact that we have experimentally demonstrated, for the first time, energy proximity of electrical and optical gaps in single molecular structures. In addition, we have developed a new metrology approach for molecular nanoelectronis that is based on the proximity of electrical and optical gaps.

ACKNOWLEDGEMENT

We are very grateful for the advices, notes and corrections we receive from our four anonymous reviewers.

COMPETING INTERESTS

Authors have declared that no competing interests exist.

REFERENCES

1. Aradhya SV, Venkataraman, L. Single-molecule junctions beyond electronic transport. Nature Nanotechnology. 2013;8:399–410. DOI:10.1038/nnano.2013.91
2. Ohnishi H, Kondo Y, Takayanagi K. Quantized conductance through individual rows of suspended gold atoms. Nature. 1998;395:780–783.
3. Salomon A, Cahen A, Lindsay SM, Tomfohr JK, Engelkes VB, Frisbie CD. Comparison of electronic transport measurements on organic molecules. Adv Mater. 2003;15:1881–1890. DOI: 10.1002/adma.200306091
4. Vilan A. Analyzing molecular current-voltage characteristics with the Simmons tunneling model: scaling and linearization. J. Phys. Chem. C. 2007;111:4431-4444 DOI: 10.1021/jp066846s.

5. Akkerman HB, Naber RCG, Jongbloed B, van Hal PA, Blom PWM, de Leeuw DM, de Boer B. Electron tunneling through alkanedithiol self-assembled monolayers in large-area molecular junctions. Proc. Nat. Academy of Science. 2007;104(27): 11161–11166. DOI: 10.1073/pnas.0701472104.
6. Wang W, Lee T, Kretzschmar I, Reed, MA. Inelastic electron tunneling spectroscopy of an alkanedithiol self-assembled monolayer. Nano-letters. 2004;4(4):643–646. DOI: 10.1021/nl052471v.
7. Beebe JM, Kim B, Gadzuk JW, Frisbie CD, Kushmerick JG. Transition from direct tunneling to field emission in metal-molecule-metal junctions. Phys. Rev. Lett. 2006;97(2):026801.
8. Beebe JM, Kim B, Frisbie CD, Kushmerick JG. Measuring relative barrier heights in molecular electronic junctions with transition voltage spectroscopy. ACS Nano. 2008;2:827–832.
9. Choi, SH, Kim, B, Frisbie CD. Electrical resistance of long conjugated molecular wires. Science. 2008;320:1482-1486.
10. Pakoulev AV, Burtman V. Temperature dependent barrier crossover regime in tunneling single molecular devices based on the matrix of isolated molecules. J. Phys. Chem. C. 2009;113:21413–21421. DOI: 10.1021/jp9056576.
11. Song H, Kim Y, Jang YH, Jeong H, Reed MA, Lee T. Observation of molecular orbital gating. Nature. 2009;462(7276): 1039-1043.
12. Pakoulev, AV, Burtman, V. Study of the transport mechanism in molecular self-assembling devices. Applied Physics A. 2010;98(4):717-734. DOI:10.1007/s00339-009-5531-5.
13. Wang W, Lee T, Reed M.A. Electron tunneling in self-assembled monolayers. Rep. Prog. Phys. 2005;68:523-544.
14. Φ_B^{LUMO} and Φ_B^{HOMO} are obtained from modeling of direct electrical measurements and therefore could be attributed to the electrically active molecular channels, i.e. to the molecules, which conduct most of the current in device at given bias.
15. CRC handbook on Chemistry and Physics, CRC Press, version, 89th Edition, Edited by David R Lide. 2008;12-114.
16. Khan MA, Xu W, Khizar-ul-Haq, Zhang XW, Bai Y, Jiang XY, Zhang ZL, Zhu WQ. Electron injection and transport mechanism in organic devices based on electron transport materials. Journal of Physics D: Applied Physics. 2008;41(22):225105. DOI:10.1088/00223727/41/22/225105.
17. Cohen R, Zenou N, Cahen, Yitzchaik S. Molecular electronic tuning of Si surfaces. Chem. Phys. Lett. 1997;279:270-274.
18. Gershevitz O, Sukenik CN, Ghabboun J, Cahen D. Molecular monolayer-mediated control over semiconductor surfaces: Evidence for molecular depolarization of silane monolayers on Si/SiO. J. Am. Chem. Soc. 2003;125:4730-4731.
19. Quek SY, Choi HJ, Louie SG, Neaton, JB. Length dependence of conductance in aromatic single-molecule junctions. Nano Lett. 2009;9(11):3949–3953. DOI: 10.1021/nl9021336.
20. Donhauser ZJ, et al. Conductance switching in single molecules through conformational changes. Science. 2001;292(5525):2303-2307. DOI: 10.1126/science.1060294.
21. Chen J, Reed MA. Electronic transport of molecular systems. Chemical Physics. 2002;281(2-3):127–145.
22. Selzer Y, Cabassi MA, Mayer TS, Allara DL. Temperature effects on conduction through a molecular junction. Nanotechnology. 2004;15(7):S483–S488.
23. Oliver B, Nowak J. Temperature and bias dependence of dynamic conductance—low resistive magnetic tunnel junctions. J. Appl. Phys. 2004;95(2):546-550. DOI: 10.1063/1.1631074.
24. Santos TS, Lee JS, Migdal P, Lekshmi IC, Satpati B, Moodera JC. Room-temperature tunnel magnetoresistance and spin-polarized tunneling through an organic semiconductor barrier. Physic Review Letters. 2007;98:016601.
25. Dahnovsky, Yu. Ab initio electron propagators in molecules with strong electron-phonon interaction. I. Phonon averages. The Journal of Chem. Physics. 2007;126:234111.
26. Malen JA, Doak P, Baheti K, Tilley TD, Majumdar A, Segalman RA, The nature of transport variations in molecular heterojunction electronics. Nano Lett. 2009;9:3406–3412.
27. Ward DR, Halas NJ, Ciszek JW, Tour JM, Wu Y, Nordlander P, Natelson D. Simultaneous measurements of electronic conduction and Raman response in molecular junctions. Nano letters. 2008;8(3):919-924.

DOI: 10.1021/nl073346h.
28. Ramachandran GK, Hopson TJ, Rawlett AM, Nagahara LA, Primak A, Lindsay SM. A bond-fluctuation mechanism for stochastic mechanism in molecular wires. Science. 2003;300:1413-1416.
29. Burtman V, Hukic G, Ndobe AS, Drori T, Vardeny ZV. Electrical and optical studies of gap states in self-assembled molecular aggregates. J. of Appl. Phys. 2007;101:054502.
30. Burtman V, Ndobe AS, Vardeny ZV. Transport studies of isolated molecular wires in self-assembled monolayer devices. J. of Appl. Phys. 2005;98:034314.
31. Burtman V, Ndobe AS, Vardeny ZV. Studies of single molecule charge transport using devices based on self-assembled monolayers. Solid State Commun. 2005;135:563-573.
32. Burtman V. Transport Studies in Molecular Devices, In book: Molecular Self-Assembly: Advances in Chemistry, Biology and Nanotechnology, Edition: 1st, Chapter: Chapter 6: Molecular Orbital Gap Studies in Tunneling Single Molecular Devices, Publisher: Nova Scientific Publisher House, Editors: James P. Comrie. 2011;183-212.
33. Simmons JG. Generalized formula for the electric tunnel effect between similar electrodes separated by a thin insulating film. J. Appl. Phys. 1963;34(6):1793-1803.
34. Simmons JG. Conduction in thin dielectric films. J. Phys. D. 1971;4:613-614. DOI:10.1088/0022-3727/4/5/202.
35. Reed MA, et al. The Electrical Measurement of Molecular Junctions. Molecular Electronics: Science and Technology, Molecular Electronics: Science and Technology, Ann. N.Y. Acad. Sci. 1998;852:133-144.
36. Holmlin RE. et al. Electron transport through thin organic films in metal--insulator--metal junctions based on self-assembled monolayers. J. Am. Chem. Soc. 2001;123:5075−5085.
37. Petta JR, Slater SK, Ralph DC. Spin-Dependent Transport in Molecular Tunnel Junctions. Phys. Rev. Lett. 2004;93: 136601. DOI:http://dx.doi.org/10.1103/PhysRevLett. 93.136601.
38. Vilan A, Hikmet RAM. Quantification of ready-made molecular bilayer junctions having large structural uncertainty. J. Phys. Chem. C. 2008;112:269-281. DOI: 10.1021/jp0755490
39. Aswal DK, Lenfant S, Guerin D, Yakhmi JV, Vuillaume D. Fowler–Nordheim tunnelling and electrically stressed breakdown of 3-mercaptopropyltrimethoxysilane self-assembled monolayers. Nanotechnology. 2005;16(12):3064-3068. DOI:10.1088/0957-4484/16/12/056.
40. Burtman V, Vardeny ZV. Design and characterization of novel systems for molecular nanoscale self-assembly. Jap J. of Appl. Phys. 2008;47:1165-1172. DOI: 10.1143/JJAP.47.1165.
41. Wang W, Lee T, Reed MA. Mechanism of electron conduction in self-assembled alkanethiol monolayer devices. Phys. Rev. B. 2003;68:035416.
42. Melvin L. The Franck-Condon Principle and Its Application to Crystals. J. of Chem. Phys.1952;20:1752-1760. DOI:10.1063/1.1700283.
43. Zahid F, Ghosh AW, Paulsson M, Polizzi E, Datta S. Charging-induced asymmetry in molecular conductors. Phys. Rev. B. 2004;70:245317. DOI:http://dx.doi.org/10.1103/PhysRevB.7 0.245317.
44. Ulman A. Formation and Structure of Self-Assembled Monolayers. Chem Rev. 1996;96:1533-1554.
45. Petelenez, P Charge trasfet excitations in organics, in Organic Nanostructures: Science and Applications, edited by VM Agranovich, GC La Rocca. ISBN 1586032712. 2002;1-21.

Peer-review history:
The peer review history for this paper can be accessed here:
http://www.sciencedomain.org/review-history.php?iid=835&id=33&aid=7592